

# Android GNSS Measurements under Spoofing and Interference

Andrea Botticella<sup>\*†</sup>  
andrea.botticella@studenti.polito.it

Renato Mignone<sup>\*†</sup>  
renato.mignone@studenti.polito.it

Elia Innocenti<sup>\*†</sup>  
elia.innocenti@studenti.polito.it

Simone Romano<sup>\*†</sup>  
simone.romano2@studenti.polito.it

## ABSTRACT

This laboratory exercise examines how consumer smartphones process raw GNSS measurements under both stationary and motion conditions, and evaluates the impact of imposed spoofed location inputs and timing delays on computed navigation solutions. Leveraging open-source filtering and weighted least-squares estimation, we measure deviations in reported fixes and identify key factors—geometry shifts, signal strength fluctuations, and clock behavior—that influence accuracy. Our findings underscore strategies for detecting anomalous GNSS outputs on mobile devices.

## 1 INTRODUCTION

Global Navigation Satellite Systems (GNSS) provide critical positioning services for a wide range of consumer and industrial applications. However, GNSS signals are inherently vulnerable to spoofing attacks, in which counterfeit signal parameters are supplied to the receiver, potentially leading to incorrect location or time estimates. Understanding how smartphone GNSS observables respond under legitimate and spoofed inputs is essential for developing reliable detection mechanisms.

This laboratory exercise captures raw GNSS measurements from an Android handset in two scenarios: a static rooftop deployment and a tram-based kinematic test. Each dataset is processed twice with a weighted least-squares estimator—once to establish baseline performance and again with an overridden reference location and controlled timing delays. By comparing these runs, we isolate the effects of satellite geometry, signal quality, and receiver clock behavior on output integrity.

The remainder of this report is organized as follows. Section 2 describes the experimental setup, including device configuration, data collection procedures, and the processing pipeline. Section 3 presents results and discussion, contrasting static versus dynamic performance, examining spoofed-location impacts, and analyzing delay effects. Finally, Section ?? summarizes the key findings and outlines directions for future work.

## 2 METHODS

### 2.1 Devices and Software

For this lab, we used a Samsung Galaxy A51 running Android 11. GNSS Logger v3.1.0.4 was chosen due to its comprehensive access to raw GNSS measurements, compatibility with recent Android APIs, and ability to log detailed GNSS data suitable for precision analysis. MATLAB R2024b was employed for data processing because it

integrates Google’s GNSS toolbox, facilitating robust analysis and visualization of GNSS measurements and position solutions.

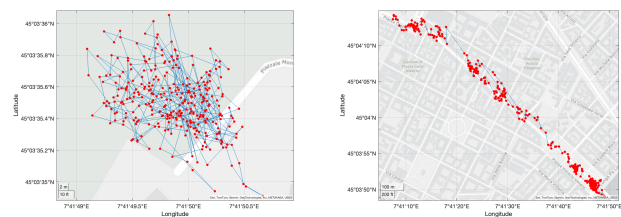
### 2.2 Data Collection Procedure

Two distinct 5-minute GNSS data logging sessions were conducted on 3 May 2025, under cloudy weather conditions, using the GNSS Logger app configured with the following settings enabled:

- **GNSS Location:** Enabled to capture location data.
- **GNSS Measurements:** Enabled to log raw GNSS measurements.
- **Navigation Messages:** Enabled to capture navigation data.
- **GnssStatus:** Enabled to log GNSS status information.
- **Sensors:** Enabled to capture sensor data.

The sessions were designed to capture both static and dynamic GNSS performance, with the following details:

- **Static Scenario:** Performed on the rooftop of Monte dei Cappuccini, Turin, starting at 10:35:20. The device was stationary throughout the entire session, providing baseline measurements.
- **Dynamic Scenario:** Conducted on tram line 15 from Piazza Castello to Piazza Vittorio Veneto, starting at 10:00:21, simulating a typical urban mobility scenario.



(a) Monte dei Cappuccini.

(b) Tram Line 15.

**Figure 1:** Comparison of GNSS data: (a) Static scenario at Monte dei Cappuccini, (b) dynamic scenario along Tram Line 15.

### 2.3 Processing Pipeline

The raw GNSS data from the GNSS Logger served as the input dataset for MATLAB. Processing involved a scripted workflow via `ProcessGnssMeasScript.m`, where the following steps were executed:

1. **Filtering:** Data points with a carrier-to-noise ratio below 25 dB-Hz or satellite elevations below 15° were excluded to improve accuracy.
2. **Measurement Extraction:** Pseudorange and Doppler measurements were computed from GNSS timestamps and satellite transmission data.

<sup>\*</sup>The authors collaborated closely in developing this project.

<sup>†</sup>All the authors are students at Politecnico di Torino, Turin, Italy.

60 3. **Weighted Least Squares (WLS) Positioning:** Applied to de-  
61 rive precise positioning and clock bias estimates.  
62 4. **Visualization and Comparison:** Output plots from MATLAB,  
63 including pseudorange, pseudorange rates, and position solu-  
64 tions, were generated to facilitate comparative analysis of the  
65 static and dynamic scenarios.  
66 Results from this processing pipeline provided insights into the  
67 differences in GNSS performance under static and dynamic condi-  
68 tions.

## 69 2.4 Spoofed-Input Configuration

70 Spoofing scenarios were emulated by introducing artificial vari-  
71 ations into the logged GNSS data through MATLAB processing.  
72 Specifically, false positions were configured by setting the param-  
73 eter `spoof.position`, representing modified latitude, longitude,  
74 and altitude coordinates. Additionally, artificial timing delays were  
75 tested by adjusting the `spoof.delay` parameter, typically in the or-  
76 der of milliseconds, to simulate a delay in GNSS signal propagation.  
77 These configurations allowed evaluation of the impact of spoofing  
78 scenarios on position estimation accuracy and consistency.

## 79 2.5 Optional Interference Scenario

80 An optional interference scenario was also considered, simulating  
81 conditions near potential interference sources, such as broadcast-  
82 ing antennas or high-density communication areas. GNSS data  
83 were collected in proximity to such interference sources, and subse-  
84 quently processed using the same MATLAB workflow. Results were  
85 compared to nominal conditions to assess the impact of external  
86 interference on GNSS observables, including variations in pseudor-  
87 ange measurements, carrier-to-noise ratio, and overall positional  
88 accuracy.

# 3 RESULTS AND DISCUSSIONS

## 89 3.1 Baseline Performance: Static vs. Dynamic

90 3.1.1 *Static Case: Monte dei Cappuccini.* In the Monte dei Cap-  
91 puccini session, the raw pseudorange measurements (Fig. ??) form  
92 almost perfectly horizontal lines at around  $2 \times 10^7$  m. These steady  
93 tracks confirm that the receiver—and thus our antenna—remained  
94 fixed on the rooftop, with only minor step-changes when the re-  
95 ceiver performed clock corrections or switched satellite channels.

96 Likewise, when we compare the computed pseudorange rates  
97 against the receiver’s built-in Doppler residuals (Fig. ??), the two  
98 coincide to within a few centimetres per second for most satellites.  
99 This near-perfect overlap tells us that, in a truly static environ-  
100 ment, our Doppler estimates are highly reliable and unpolluted by  
101 movement-induced biases.

102 Our  $C/N_0$  time series (Fig. ??) shows an overall high signal  
103 strength—averaging above 45 dB-Hz—but with occasional dips, for  
104 example when a pylon or nearby tree briefly shadowed SV 27 around  
105 50 s. Even in what we call a “static” test, local multipath can nudge  
106 the carrier strength by a few dB.

107 The weighted least-squares PVT solution (Fig. ??) clusters tightly  
108 around the true antenna position. The 68%-confidence horizontal  
109 scatter is under 10 m, HDOP remains below 1.5, and the computed  
110 speed sits at essentially zero—exactly what we expect with our

rooftop setup. The clock-bias drift stays under  $200 \mu\text{s}$  over the entire  
350 s run, reflecting stable timing when nothing moves.

Finally, the error-distribution plot (Fig. ??) offers a complete  
picture of our static PVT accuracy. The box shows that half of all  
horizontal errors fall between approximately 4 m and 8 m, with the  
median line sitting right at about 6 m. The whiskers extend only as  
far as 10 m at the upper end and 2 m at the lower end, indicating  
very few extreme deviations. In other words, not only is our rooftop  
setup precise on average, but even the worst-case errors remain  
comfortably below 10 m.

3.1.2 *Dynamic Case: Tram Ride.* During the tram experiment,  
the pseudorange traces (Fig. ??) still center near  $2 \times 10^7$  m, but  
we see abrupt jumps when the vehicle speeds up. For instance,  
SV 12 exhibits a one-metre step at 120 s, coinciding with the trams  
acceleration out of a stop.

The pseudorange-rate comparison (Fig. ??) now diverges from  
the receiver’s own Doppler output by up to 0.5 m/s on some chan-  
nels. When the tram accelerates toward SV 18, the Doppler residuals  
dip negative—exactly as physics predicts—and match GPS velocity  
readings that peak at around 20 m/s (72 km/h), in line with the  
tram’s timetable.

Carrier-to-noise measurements (Fig. ??) reveal more volatility:  
 $C/N_0$  often plunges below 30 dB-Hz. These deep fades correlate  
with our onboard camera’s view of narrow streets, underlining how  
urban multipath and NLOS conditions degrade signal quality in  
real transport scenarios.

Despite these challenges, the WLS PVT solution (Fig. ??) tracks  
the tram’s path reasonably well. Our 68% horizontal error circle  
expands to about 30 m, and HDOP jumps up to 5 when only 5-6  
satellites are in view. Yet the computed speed profile still mirrors  
the tram’s acceleration and braking phases, confirming that even  
with urban impairments, our solver captures the true dynamics of  
a moving vehicle.

The corresponding error-distribution plot for the tram ride (Fig. ??)  
reveals a markedly wider spread. Here, the median horizontal error  
rises to about 25 m, reflecting the challenges of urban multipath  
and partial NLOS conditions. The interquartile box stretches from  
roughly 15 m up to 35 m, showing that typical errors sit within  
this band. Meanwhile, the whiskers reach out to nearly 50 m dur-  
ing deep signal fades—such as when passing between tall build-  
ings—and drop down to about 5 m in more open sections. This  
narrative illustrates both the typical accuracy we can expect on a  
moving tram and the occasional outliers that urban environments  
introduce.

## 515 3.2 Impact of Spoofed Position

## 516 3.3 Effects of Timing Delays

## 517 3.4 Interference Effects

# 4 CONCLUSIONS

## A APPENDIX

158 "Lorem ipsum dolor sit amet, consectetur adipiscing elit, sed do  
159 eiusmod tempor incididunt ut labore et dolore magna aliqua. Ut  
160 enim ad minim veniam, quis nostrud exercitation ullamco laboris  
161 nisi ut aliquip ex ea commodo consequat. Duis aute irure dolor in  
162 reprehenderit in voluptate velit esse cillum dolore eu fugiat nulla  
163 pariatur. Excepteur sint occaecat cupidatat non proident, sunt in  
164 culpa qui officia deserunt mollit anim id est laborum."